Spring 5-1-2009

Measuring Dose to Small Animals in Micro-CT

Avi Hameroff

Abstract

An important application of William Röntgen's discovery of x-rays is computed tomography (CT). First developed in the 1970's, CT scanners of today are able to provide a detailed image of a patient's body with minimal risk to patient and a very short turnaround time from scan to reconstructed image. This powerful tool provides physicians another way to diagnose patients while simultaneously allowing for researchers to learn about the human body.

Scientists soon became interested in using the technology on small animals but practical issues plagued the widespread use of CT in preclinical research. The scale of the scanners was simply too large to provide useful images of the animals, mainly mice and rats. As a direct result of this problem, the field of micro-CT was developed. Micro-CT scanners can be used to generate images of small animals in while the platform itself has been used to develop advancements applied to clinical CT.

In February 2006, the Syracuse Medical Imaging Research Group (SMIRG) acquired a Siemens Micro CAT II scanner. At the time, only theoretical predictions of dose to small animals existed and they were based in part on computer models.

It became necessary to perform a dosimetry study of the micro-CT scanner in order to empirically determine the dose to small animals during a scan. Utilizing materials and the method outlined by the SUNY Upstate Medical University Department of Radiation Safety, the study was successfully completed in May 2008. In order to measure exposure, thermoluminescent dosimeters (TLDs) were calibrated using an ionization chamber and then exposed in-air to obtain conversion factors. The TLDs were then exposed inside of a phantom. Post phantom exposure measurements were converted into kerma measurements which were finally converted into dose estimates using the f-factor for mice.

Mathematical equations which can predict dose estimates to small animals during scanning were developed. The equations, one for each of three filter thicknesses, allow the researcher to input their scan's technique (peak voltage and current applied to the tube, and exposure time) and obtain an empirically-derived prediction of dose to the subject. This project provided a powerful tool to researchers and proved that dose to animals during micro-CT scanning, while small, is not insignificant. In addition, it also validated earlier dose predictions which were developed using computer models.

Table of Contents

Acknowledgements

I would first and foremost like to thank Russell Kincaid for taking me under his wing and teaching me almost everything I know about medical imaging. Before I was assigned my own project, he allowed me to work with him and he showed me around the lab, teaching me about the micro-CT scanner and helping me to get started. I also would like to thank Marsha Roskopf for teaching me about TLDs and how to properly handle and read them. Her willingness to guide and teach me how to use the instruments in the Radiation Safety office were vitally important to the completion of this project and for all of her help, I thank her.

In addition, thanks to my advisors Edward Lipson and Andrzej Krol for providing me with the experience to work in a medical imaging lab and for showing me a glimpse of the cutting edge of radiology. It has been a pleasure working with them both and I look forward to reading about the future accomplishments of the group (and implementing them as a radiologist). The copy of The Physics of Radiology, which I used extensively during my independent study, was given to me by Professor Lipson. With my Capstone complete, it will now serve as the foundation of my collection of medical textbooks.

Of course, none of this would be possible without the support and assistance of the Honors program and advisors Carolyn, Steve, Hanna, Eric, Marilyn, Vicki, and Dr. Gorovitz. Thank you all for being there for me as I grew into the student and person I am today. Your willingness and ability to support my success helped my growth tremendously and for that I am very grateful. And to think, it was almost exactly four years ago when Carolyn made the phone call to my house, informing me that I had been accepted in to the Honors program. I think you made a great choice!

Finally, many thanks to the custodial staff of SUNY Upstate for providing me with company and coffee during those long, late nights of seemingly endless scanning.

Advice to Future Honors Students

As I reflect on my time spent completing my Capstone project, I can honestly say that the most important word of advice I can offer is the following: do your actual work/research early!

While the majority of the writing associated with my project was completed during this past year, all of the research was actually conducted almost two years prior. The hardest part was remembering what exactly I had done and where I had placed all of my data. There was no frantic last-minute scanning to be completed, much to my delight. Instead, I was able to spend some of my free time during my senior year pursuing really interesting courses (like the HNR 340 anthropology course in which I danced a traditional Vietnamese dragon dance) and doing what I enjoy most, teaching.

Due to the craziness that is known as the end of senior year, I was not able to submit my Capstone on time but that wasn't because there was any more research to be performed. In the final two weeks of prepping, I became caught up in school and outside work, sacrificing precious Capstone-writing time in order to learn the Vietnamese dragon dance, prep students for their organic chemistry exam, and organize a magic show.

Therefore, I urge you, future Honors student, to get in touch with a professor who interests you and begin your scholarly pursuit as early as possible. That way, when you reach your senior year and find yourself caught up with multiple time-consuming commitments, the Capstone project won't seem so daunting. Hopefully, you'll even be able to do a better job of time management and actually complete your writing on time. If not, no worries- I am still breathing, and I am confident that the sun will still shine (eventually… this is Syracuse don't forget!).

Another slight worry I had while working on my Capstone was that it wasn't very interesting or original. If you find yourself in a similar predicament, I urge you to take a step back and consider the big picture. Reflect on the work you're doing and realize that if you've been approved to write a Capstone and have a professor who wants to sign their name to your project, it most certainly is significant and meaningful, which is pretty amazing. For example, in my project, collecting TLD measurements wasn't the most exciting task in the world. It took a lot of time and was very tedious. But as part of my thesis work, I was operating a micro-CT scanner, worth a third of a million dollars, completely unsupervised! In addition, I was able to take some of my research time to complete an independent study in radiology and got a glimpse at what might interest me when I graduate and go on to medical school.

The reason I share this with you is that while completing my thesis, I was sometimes concerned that my work wasn't as exciting as some of my peers or that somehow it was insignificant. I too then did a bit of personal reflection and, with the help of my advisors, realized that while parts of my work weren't very exciting, my accomplishments were pretty remarkable.

So, with all that in mind, I invite you to sit back, relax, and enjoy my Capstone project. There may be parts which aren't terribly exciting, but the project as a whole was successful and I am very proud of it. The research that you will be reading about was completed almost exclusively on my own and the following thesis report was similarly compiled independently, of course with input and assistance from my Capstone advisor and reader.

Finally, on to my final piece of advice to you: make sure you actually complete your Honors Capstone! Even if you're not planning on pursuing any type of graduate degree, the actual experience of completing the Capstone is a great exercise in completing scholarly work and allows you to extensively study your area of interest. In my case, I received a total of 12 credits to complete my Capstone which gave me ample time to complete an independent study in radiology and learn all about micro-CT. Completing such a project entails a great deal of personal growth and I'm glad to have the experience under my belt, and so will you.

Enjoy!

Introduction

When Wilhelm Conrad Röntgen accidentally discovered x-rays in 1895, he introduced the field of physics that would become known as radiology and medical imaging. By developing the very first radiograph, he gave the world a noninvasive glimpse of the insides of the human body. Röntgen laid the foundation for medical imaging as he saw the bones and tissue beneath the skin on his wife's hand [1].

X-rays are photons (massless particles that travel at the speed of light) with a wavelength higher than 10^{-8} m and energy higher than 2×10^{-17} J [2]. One can choose x-ray energy that is ideal for use in imaging of biological systems if x-rays are able to penetrate skin but are absorbed to varying degrees by tissues inside the body. This allows them to generate clinically useful images of internal organs if detected appropriately.

These high-energy particles can also damage biological systems. As a form of ionizing energy, x-ray photons ionize atoms of material they travel through by liberating electrons through Compton and photoelectric interactions. In a photoelectric interaction, an incident photon transfers all of its energy to an atomic electron [3]. The transferred energy is great enough to allow the electron to overcome the work function of its host material and the ejected electron, known as a photoelectron, leaves with the remaining energy from the incident photon as its kinetic energy ($K = E - \phi$, where K is the resulting kinetic energy of the

photoelectron, E is the energy of the incident photon, and ϕ is the work function of the material). In a Compton interaction, only some of the incident photon's energy is used to liberate an atomic electron. The remaining energy scatters as a lower-energy photon [3]. These electrons can then repeat the process in a cascading fashion until the electrons no longer have enough kinetic energy to do so. Because soft x-rays have lower energy, their interactions occur over larger areas resulting in an increased possibility that incident electrons could damage DNA. The distance that these cascading interactions occur over as a function of electron energy is given by the linear energy transfer (LET) function, with soft x-rays having high LET values [2].

When x-rays were first used for human imaging, the mechanism through which they can cause cancer was not understood nor appreciated, and morbidity related to radiation dose resulted. Dose is a measure of energy per unit mass that is actually deposited in matter through the Compton and photoelectric processes. Because such a measurement is difficult to obtain directly, dose is calculated based on measurements of exposure, which is defined as the "amount of ionization charge liberated per unit mass of air irradiated," (Wolbarst, 1993, p. 96). The SI unit of exposure therefore is Coulomb per kilogram (C/kg), with conventional unit Roentgen (R) where $1\ R = 2.58 \times 10^{-4}$ C/kg. Exposure measurements can be made using an ionization chamber and, because of the linear relationship between exposure and air kerma (kinetic energy released in matter), they can be converted into measurements of kerma and finally to estimates of

dose [2]. The two quantities are related by the *f* factor, which takes into consideration the way in which tissue absorbs energy [4].

Today, x-ray production for clinical applications (with the exception of mammography) still uses the highly inefficient Brehmsstrahlung (translation: braking radiation) process. In this process, a metal cathode usually made of tungsten is heated so that electrons in the valence shell are energized and leave an atom of the metal with high energy, attracted to the positively charged anode. Upon reaching the anode, the electrons rapidly undergo a change in velocity (acceleration) as they interact with an atom of the anode, causing the release of a photon [2]. Under appropriate conditions, the photon emitted will have enough energy to be classified as an x-ray.

This generation process severely limits the x-ray photon fluence (i.e. number of photons per time unit and per unit area) and produces a broad energy spectrum, resulting in longer scans and suboptimal patient dose [5]. This is primarily because, when the electrons leave the cathode material, they will travel along the potential gradient established. The potential gradient is established as part of the scan's technique, which includes the peak voltage (in units of kVp) applied across the x-ray tube, the current applied to the tube (in units of mA) and the exposure time (seconds) of CT scan. Because the established potential gradient is only the maximal gradient, x-rays leave the anode with varying energies only capped by this setting. For this reason, not all electrons will be able to produce x-rays, let alone x-rays with a specific energy. In practice, as much as 99% of the energy, which could potentially be converted into useful x-ray photons

is lost as heat [2]. To add to the inefficiency of current x-ray production, soft x-rays, which have lower energy and characteristics similar to ultraviolet radiation, are filtered out by a metal filter placed in front of the x-ray source, because of their increased ability to cause cancer [2]. The filter must be changed in order to appropriately match the specific imaging task. For example, on the micro-CT system being considered in this study, a 1 mm aluminum filter would prohibit most (if not all) x-rays generated by a scan at 50 kVp. For the scanner we used (MicroCAT II) the process of filter change is difficult, requiring disassembly of the scanner and there is serious risk of x-ray source damage if done improperly.

By using an ultrafast laser based x-ray source (ULX), made possible by chirped-pulse amplification (CPA) [10], the Syracuse Medical Imaging Research Group (SMIRG) is hoping to produce a higher fluence of x-ray photons with narrower energy spectrum originating from a smaller focal spot [5]. If successful, this new source will allow reduction of scan duration while increasing image contrast and resolution. In addition, ULX technology could usher in a new era of CT technology known as phase-contrast imaging which has the advantage of being able to distinguish tumors from soft tissue. Phase contrast calls for spatial coherence of the x-rays, which essentially means that they originate from an approximate point source. This is not currently possible with conventional methods but could be achieved by generating the x-rays using laser [11]. CPA works by using a commercially available compact, tabletop laser to generate a beam. The laser beam is then spectrally “stretched” and amplified. Finally, the beam is spectrally compressed so that the resulting beam has the same pulse

duration as the original, but can have energy that is approximately 10 orders of magnitude greater [5].

CPA is the key technology enabling ULX as it allows for high power density (10^{18}-10^{20} W/cm^2) to be delivered to a target material using readily available terawatt (10^{12} W) lasers with femtosecond (10^{-15} s) range pulse durations [5]. This technology is being intensely investigated because of its many practical applications. There is no anode, so overheating of target materials does not occur and a wide variety of materials can be used, allowing for better matching to the imaging project at hand. Furthermore, target materials can be switched quickly and effortlessly. The process also has the advantages of emitting x-rays with a narrow spectrum and decreasing the focal spot size to as low as 2 μm [5]. Scans performed in this fashion are preferred because the photons have lower LET values, scans are much quicker, and image spatial resolution is greatly improved due to the smaller focal spot.

As an example of a practical application of this new technology, the research group has chosen the computed tomography (CT) imaging modality upon which to evaluate their claims of reduced dose using the ULX technology. In computed tomography, the computer is essential in reconstructing a two-dimensional image from raw data, which does not correlate in any useful way to an image. CT acquires one 2D image (view) at a time. This process is then repeated until a full 360-degree rotation about the patient or specimen has been complete and a large number of views are acquired [2]. The image is then reconstructed from this set of data with each coefficient corresponding to a

specific pixel shade as defined by the CT number. The CT number scale ranges from –1000 for air to 1000 for bone and is centered at 0 for water. Because of the wide range, the image grayscale is often calibrated depending on the specific imaging task, resulting in an image with more contrast over a narrower range. This can highlight varying soft tissue, for example, and allows researchers and physicians to obtain vital information, which can then be used to treat illness.

Motivation

The SMIRG and other research groups are interested in focusing on micro-CT because of its widespread use and smaller scale which better allows for novel developments to be implemented, as compared to clinical scanners. Imaging of small animals (mice and rats) using micro-CT can be used to study tumor growth and the micro-CT itself can be used as a platform upon which to further develop the CT technology for application in the clinical sector. For example, the group (SMIRG) is using the platform of the micro-CT to develop their ULX technology and compare it to the conventional method of x-ray production. Both implementation and evaluation are easier and more cost-effective on the smaller scale of the micro-CT. It is also significantly less laborious to test, and animal subjects are easily attainable for imaging studies. Once thoroughly developed and tested, the group is then hoping to partner with industry in order to bring ULX technology into the preclinical and clinical sectors.

In addition, this work was necessary because in February 2006, when SMIRG acquired a Siemens Micro CAT II scanner (Fig. 1), only theoretical predictions of dose to small animals existed and they were based in part on computer models. Also included with the software of the micro-CT scanner was a "dose calculator" provided by Siemens, but it was unclear what its dose predictions were based on.

For reasons highlighted previously, it became necessary to perform a dosimetry study of the micro-CT scanner in order to empirically determine the dose to small animals during a scan.

Figure 1: The Siemens Micro-CAT II with adjacent image processing station [6]

Methods

As previously discussed, exposure measurements can be made directly by using an ionization chamber (Fig. 2). The ionization chamber contains a parallel plate capacitor. As air molecules are ionized, the positively charged molecule will be attracted to the negatively charged plate while the liberated electrons will move towards the positive plate. This movement can be detected and is reported as a measurement of exposure in units of roentgen.

Figure 2: The MDH Industries Model 1015 radiation monitor used in this study with the 10X5-6 ion chamber attachment disconnected, housed in the instrument's cover [7]

Measurements of exposure can then directly be converted into estimates of dose through use of the *f* factor, but as a practical matter, it is exceedingly difficult to obtain exposure measurements inside of a biological specimen. This is mostly due to the diameter of the ion chamber, which is large compared to the diameter of a small animal. Therefore, thermoluminescent dosimeters (TLDs) are

used in conjunction with phantoms to obtain desired exposure measurements. A description of thermoluminescent dosimeters follows: "Luminescent materials typically are insulator salts that have been highly purified and then, when in molten form, doped with precise amounts of special impurities. The impurities create discrete quantum states, somewhat like orbitals of free atoms, with energies lying in the forbidden band or band gap between the (nearly filled) valance band and the (practically empty) conduction band of the host material... Such a state, called an *electron trap*, is capable of holding one electron" (Wolbarst, 1993, p. 134). Thermoluminescent materials emit light after they have been irradiated and then appropriately heated. They are used extensively in dosimetry studies because, after irradiation, they are stable and can hold electrons for a period of weeks.

TLDs are also small, on the order of millimeters, making them ideal for placement inside of a small animal or human phantom. A phantom is a fabricated object designed to simulate properties of biological tissue with respect to their interaction with electromagnetic radiation. Phantoms can be as simple as the one used in this study, which was a 30 mm diameter cylinder constructed of polymethyl methacrylate (PMMA). It was 10 cm long and had an insert to allow for the placement of TLDs. Phantoms can also be constructed to be more complex in order to more accurately model a larger animal or human.

The TLDs used in this study were Harshaw TLD-100s (Fig. 3) and they were read using a Harshaw model 2000A Thermoluminescence Detector and Harshaw model 2000B Automatic Integrating Picoammeter. This combination of

detector and picoammeter resulted in readings that were reported in units of current, not exposure. Therefore, it was necessary to calibrate the reported current of the ammeter so that the readings could be converted into more useful measurements of exposure. This was done through a series of in-air scans in which the ionization chamber was exposed at a certain technique and its outputted measurement of exposure was averaged over a series of three scans. A set of 30 TLDs were then exposed in identical conditions throughout three scans. The TLDs were then read and the reported values of current were recorded. A factor was then calculated to allow for direct conversion of ammeter output to exposure measurement. This was possible because current, which is charge per unit time, is directly related to exposure [4]. After this initial conversion step, it was possible to then place TLDs in animal phantoms and be able to obtain exposure measurements, which were converted into kerma measurements, and finally, dose estimates.

Figure 3: Thermoluminescent dosimeters (TLDs) in holding tray. Also pictured are "Radiation Products" TLD Suction Tweezers. These suction tweezers must be used to maintain the structural integrity of the TLDs which is key to their ability to trap electrons properly. [8]

In order to complete the study, it was necessary to place the TLDs into phantoms and image them, mirroring the technique which would be most likely used by other researchers to perform real live-animal scans. The TLDs then had to be read and annealed after being calibrated for each setting of x-ray tube voltage that was being studied. Once the dose estimates were calculated, the measurements were compared to the dose estimated using Monte Carlo simulations performed by Boone et al [9]. It was then planned to perform the study again at the INRS lab at the University of Quebec, Canada in order to measure the radiation dose of the ULX-based setup currently in development. It was expected that the application of a narrower spectrum of x-ray photons would result in lower radiation dose to the animals as compared to the conventional micro-CT scanner [5]. However, time and funding constraints did not allow for travel to Canada and technical problems have limited the pace of development of

the ULX apparatus. A comparative analysis of all acquired data to that which was predicted by previous computer simulation was performed and the results were compiled and appropriately reported.

Research Plan

Dose measurements can be calculated from the air kerma, which is an acronym for "kinetic energy released in matter" [2]. Kerma calculations, K, can be made directly from measurements of exposure, X, through the use of a conversion factor according to the equation [9]:

$$K = 0.00873\ X \qquad (1)$$

The research plan was to measure the exposure at each setting of x-ray tube filter and peak voltage of the x-ray tube, and then to irradiate and read thermoluminescent dosimeters (TLDs) under identical conditions. The TLD readings were then calibrated to exposure measurements based on the results of the “in-air” reading. After reading, the TLDs were annealed using the procedure outlined by Ogden et al [8]. The procedure was to first heat the TLDs to 400 C for one hour, allow them to cool for 30 minutes, and to heat them to 100 C for 2 hours. The TLDs were then allowed to cool overnight.

After annealing, the TLDs were placed inside of a phantom, a 30 mm diameter cylinder made of an acrylic plastic (PMMA) with an insert, which

allowed for TLD placement in the middle of the chamber. They were then irradiated again under the same scan technique, read, and annealed.

The observed TLD reading was converted to a measurement of exposure using the conversion factor obtained previously. Using equation 1, the exposure calculation was then converted into a calculation of air kerma. Finally, using the kerma-to-dose conversion factors provided by Boone et al [9], the kerma calculations were converted in to dose calculations.

For each CT scan, the x-ray tube current and exposure time was kept constant at 76 mA s (0.5 mA tube current, 8 s exposure time, 19 steps/scan). Different settings of X-ray tube filter and voltage were studied:

Filter Thickness (mm)	X-Ray Tube Voltage (kVp)
1	80, 70
0.5	70, 60, 50
0.25	50

In order to measure the exposure, an MDH Industries Radiation Monitor model 1015 was used with the 10X5-6 ion chamber attachment. The ion chamber was irradiated at each setting and its exposure measurements were used to calibrate the TLDs.

The thermoluminescent dosimeters used in this study were Harshaw TLD-100 chips that are made of lithium fluoride doped with magnesium. In order to preserve their luminescent properties, they were handled with Radiation Products

suction tweezers. The TLDs were read using a Harshaw model 2000A Thermoluminescence Detector and Harshaw model 2000B Automatic Integrating Picoammeter.

Once a measurement of dose for each setting of kVp and filter thickness was obtained, it was then planned to divide out the dependence on the tube current and exposure time in order to devise an equation to estimate dose based on the scan's technique (combination of peak voltage, current applied to the tube, and exposure time) unique to each of the three settings of X-ray tube filter.

All materials, except for the micro-CT scanner and TLDs, were provided by the Department of Radiology, State University of New York Upstate Medical University.

Results

1.0 mm Filter:

Tube Voltage (kVp)	TLD Conversion Factor (R nC^{-1})	Average Dose (mGy)	Average Dose Per Unit Current ×Exposure Time (mGy mA^{-1} s^{-1})	Average Kerma (mGy)	Average Dose Per Unit Kerma (mGy mGy^{-1})
70	0.061	26.9	0.354	30.8	0.873
80	0.059	35.6	0.468	39.5	0.901

Dose = $(0.011X - 0.444)M$
where X is the peak voltage (kVp) and M is the product of tube current and exposure time.

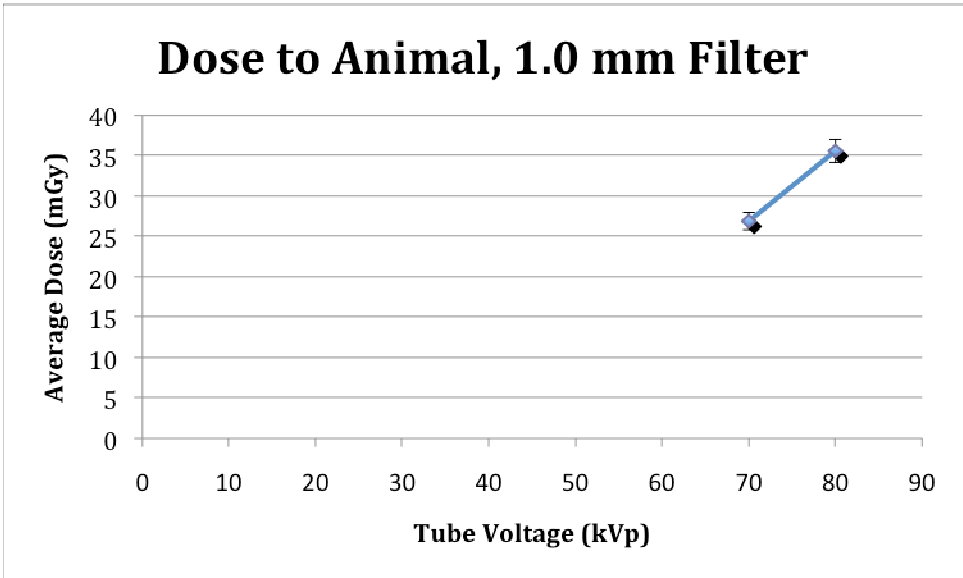

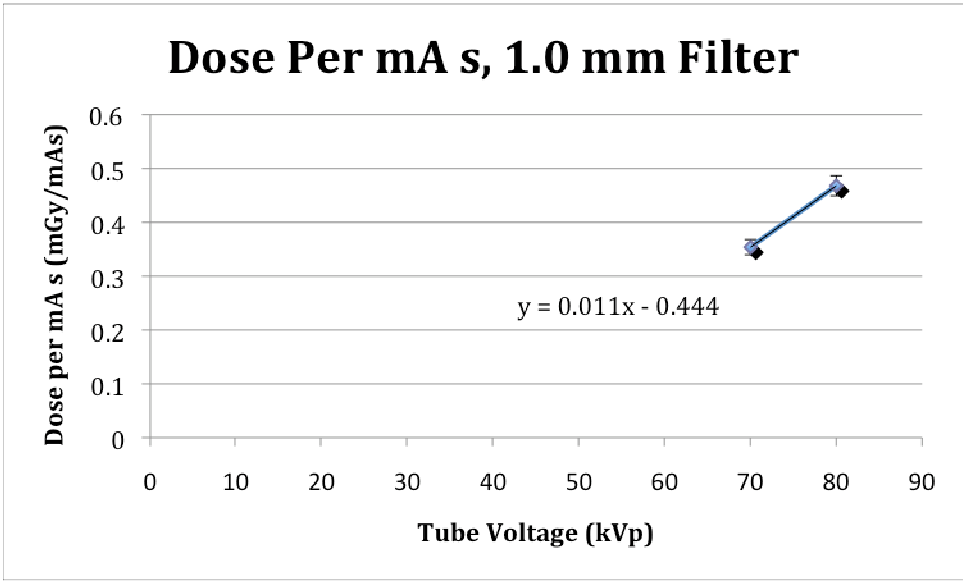

0.5 mm Filter:

Tube Voltage (kVp)	TLD Conversion Factor (R nC^{-1})	Average Dose (mGy)	Average Dose Per Unit Current ×Exposure Time (mGy mA^{-1} s^{-1})	Average Kerma (mGy)	Average Dose Per Unit Kerma (mGy mGy^{-1})
50	0.103	16.8	0.221	37.7	0.446
60	0.088	38.7	0.509	46.3	0.836
70	0.093	54.5	0.717	62.5	0.872

Dose = $(0.024X - 1.005)M$

where X is the peak x-ray tube voltage (kVp) and M is the product of tube current and exposure time.

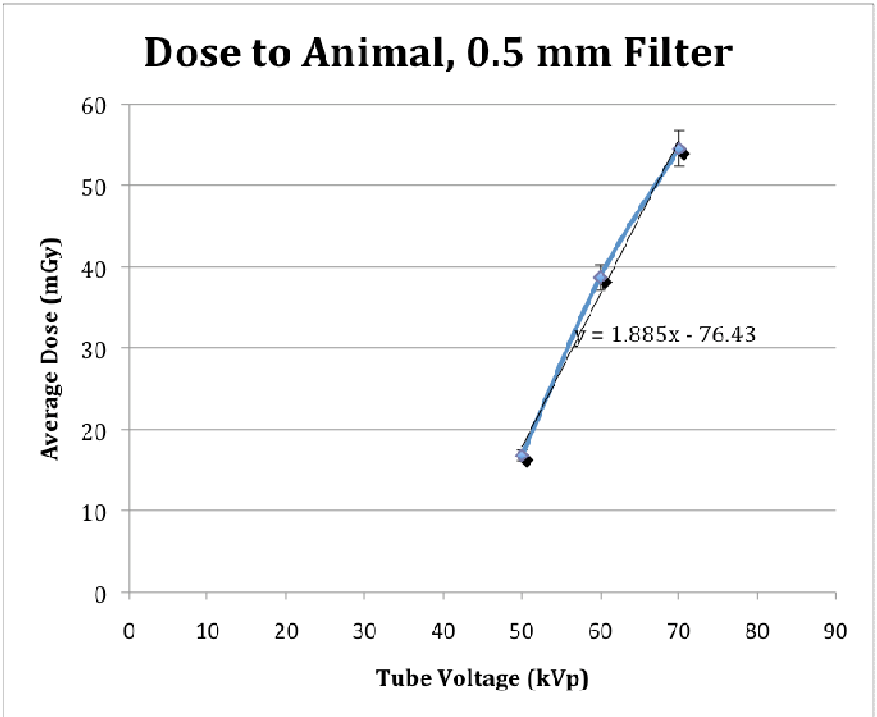

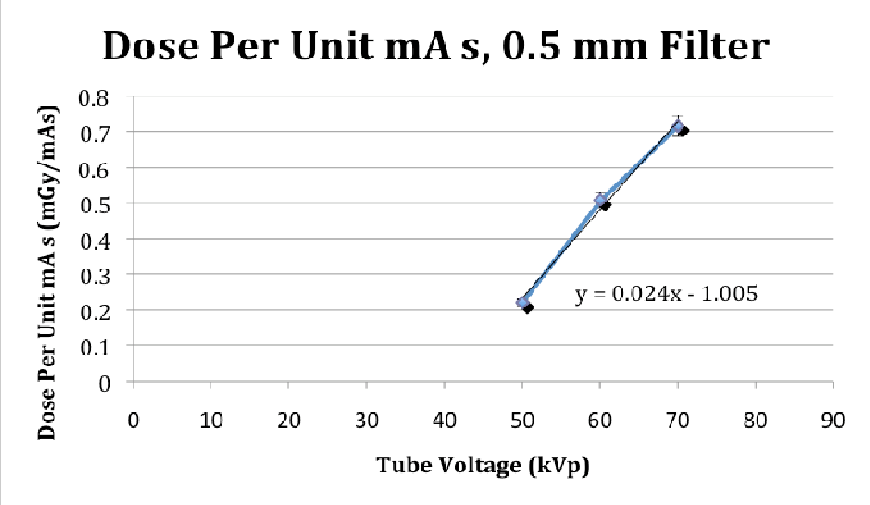

0.25 mm Filter:

Tube Voltage (kVp)	TLD Conversion Factor (R nC^{-1})	Average Dose (mGy)	Average Dose Per Unit Current ×Exposure Time (mGy mA^{-1} s^{-1})	Average Kerma (mGy)	Average Dose Per Unit Kerma (mGy mGy^{-1})
50	0.078	13.2	0.174	29.7	0.444

Dose = $0.174M$

where X is the peak x-ray tube voltage (kVp) and M is the product of tube current and exposure time.

Note: With 0.25 mm filter, only tube voltage of 50 kVp was studied. Therefore, the dose estimates provided by this study are only valid at 50 kVp.

The standard error on calculations made in this study is 5% [4,8].

Discussion

While mathematical equations to predict the dose to animals during scanning were produced, the results of this study were also compared to those published by Boone et al [9] who predicted dose to animals using a computer model. For several of the scan techniques studied, direct comparison of dose estimates was not possible because different combinations were studied. For example, Boone did not publish any results for x-ray filter setting of less than 0.5 mm, whereas this study considered that filter thickness with peak tube voltage of 50 kVp. Also, in this study, peak tube voltage settings of 60 and 70 kVp were considered at filter thicknesses of both 0.5 and 1.0 mm whereas Boone only studied those settings of peak tube voltage with 2.0 mm of filter.

Despite these limitations, comparisons were still possible and the results of this study proved to be consistent with those predictions published by Boone et al. Comparisons were made using tables 2-4 of the published paper [9]. Since the tables report mean dose to animal per unit kerma, those calculations will be compared. The diameter of the phantom used in this study was 30 mm, so only that column of data was analyzed for comparison to the results of this study. The tube current and total exposure time were kept constant at 0.5 mA and 152 sec, respectively.

At 1.0 mm filter thickness, the measured values of 0.873 and 0.901 mGy mGy^{-1} at 70 and 80 kVp respectively match almost exactly to the predictions of 0.8716 and 0.9002 mGy mGy^{-1} at filter thickness of 2.0 mm. Because the comparison study did not consider these settings of kVp at the filter thickness of 1.0 mm, an exact comparison was not possible. However, this comparison was still valid and the results were consistent with expectation that a thicker filter would allow fewer x-rays to irradiate the object and lower the measured dose.

At 0.5 mm filter thickness, the measured values of 0.446, 0.836, and 0.872 mGy mGy^{-1} at 50, 60, and 70 kVp respectively are similarly consistent with the predictions of 0.4454 (direct comparison), 0.8357, and 0.8716 mGy mGy^{-1}. While the comparison between calculated value and predicted value was direct at the setting of 50 kVp, the comparison at settings of 60 and 70 kVp was not. At the setting of 60 and 70 peak x-ray tube voltage, only filter thickness of 2.0 mm was considered. However, the results were still consistent with expectation. At the thinner filter thickness of the micro-CT as considered in this study, more x-ray is allowed to irradiate the object and slightly higher dose resulted.

At 0.25 mm filter thickness, the measured value of 0.444 mGy mGy^{-1} at 50 kVp seemed to likewise be consistent with the published prediction of 0.4454 mGy mGy^{-1} at 0.5 mm filter thickness. The measured value (with thinner filter) was slightly less than the predicted value (with greater filter), but within error, the results were still consistent with expectation.

Conclusion

After analyzing the data, I developed equations to predict the dose to an animal during a CT scan in the Siemens MicroCAT II scanner given the scan's technique. For each of the three filter thicknesses, a separate equation was compiled. At 1.0 and 0.5 mm filter thickness, an equation was compiled with a dependence on the technique, whereas at 0.25 mm filter thickness, the equation only depends on the product of x-ray tube current and exposure time. It is only valid for tube voltage of 50 kVp, as that was the only voltage studied at the 0.25 mm thickness.

By comparing these empirically obtained dose measurements to the dose predictions published by Boone et al. [9], it was possible to conclude that the results of this study were consistent with expectation. Even when direct comparison of data was not possible due to differences in combination of peak x-ray tube voltage and filter thicknesses being considered in each study, the inconsistency was resolved by observing that expected patterns were still observed. For example, it was observed that with a thicker filter, the net result at similar peak tube voltage was a reduction in dose. The tables provided by Boone et al [9] are extensive and provide further opportunity for this study to be expanded in order to more thoroughly validate predictions. However, this study provided considerable evidence to conclude that the published predictions are accurate.

This study further showed that dose to small animals during a micro-CT scan, while small, is not insignificant. This data will also be used in a future study to compare the dose to animals during a CT scan utilizing the new x-ray generation technique being developed by the research group. The method will use an ultrafast laser-based x-ray source (ULX) in conjunction with chirp-pulsed amplification (CPA) in order to generate x-rays in a way that is more efficient while delivering smaller dose to the animal.

References

[1]: Stevenson, A.W., Gao, D, Gureyev, T.E., Pogany, A., Wilkins, S.W. (1997). "Phase-Contrast Imaging Using Hard X-Rays." *Materials Australia.* **29:** 14-17.

[2]: Wolbarst, A.B., 1993, *Physics of Radiology*, Appleton & Lange, Norwalk, 461 p.

[3]: Thornton, S.T. and Rex, A., 2005, *Modern Physics*, Brooks Cole, Florence, 672 p.

[4]: Prof. Kent Ogden, Dept of Radiology, Upstate Medical University, personal communication

[5]: Krol, A., Kieffer, J. C., Nees, J., Chen, L., Toth, R., Hou, B., Kincaid, R. E. Jr., Coman, I. L., Lipson, E. D., Mourou, G. 2004. Ultrafast laser-based micro-CT system for small-animal imaging, Proc. SPIE 5368:265-271 (Medical Imaging 2004: Physics of Medical Imaging; Yaffe, M. J., Flynn, M. J., eds.).

[6]: MIPS Facilities-SC13, *Small Animal Imaging Resource Stanford Center for Innovation and In-Vivo Imaging (SCI^3)*, http://mips.stanford.edu/public/instruments.adp

[7]: RADCAL: 1015, *Radcal Corporation*, http://www.radcal.com/1015.html

[8]: Ogden, K.M., Lavallee, R., Huda, W., Roskopf, M.L., Scalzetti, E.M. (2005). Calibration of TLD Chips to Maximize Precision in Radiographic Phantom Dosimetry.

[9]: Boone, J.M., Velazquez, O., Cherry, S.R. (2004). Small-Animal X-ray Dose from Micro-CT. *Molecular Imaging*. **3**:149-158.

[10]: Brabec, T., and Kapteyn, H., 2009, *Strong Field Laser Physics*, Springer, New York, 591 p.

[11]: Kincaid, R., Krol, A., Fourmaux, S., Kieffer, J.-C., Serbanescu, C., Servol, M., Vogelsang, L., Wilkins, S., Stevenson, A., Nesterets, Y., Lipson, E., Ye, H., Pogany, A. 2008. Development of ultrafast laser-based x-ray in-vivo phase-contrast micro-CT beamline for biomedical applications at Advanced Laser Light Source (ALLS), Proc. SPIE 7078, 707818 (2008), DOI:10.1117/12.79554

Appendix

Table 1: Data acquired with Micro-CT X-Ray Tube Filter Thickness of 0.25 mm

Notes: To calculate the air kerma, the F factor was: 0.00873 mGy mR^{-1}

To calculate dose, the conversion factors used were:

0.4454 mGy mGy^{-1} at 50 kVp

TLD	Peak Tube Voltage (kVp)	Reading (nC)	Converted Exposure (R)	Calculated Air Kerma (mGy)	Calculated Dose (mGy)	In-Air Reading (nC)	TAR
31	50	42.5	3.32	29	12.9	61.9	0.687
32	50	41	3.2	27.9	12.4	60.9	0.673
33	50	44.5	3.47	30.3	13.5	61.6	0.722
34	50	38.9	3.03	26.5	11.8	61.1	0.637
35	50	42.5	3.32	29	12.9	61.4	0.692
36	50	38.8	3.03			57.9	0.67
37	50	41.6	3.24	28.3	12.6	53.3	0.78
38	50	43.7	3.41	29.8	13.3	58.7	0.744
39	50	45.8	3.57	31.2	13.9	55.8	0.821
40	50	43.3	3.38	29.5	13.1	57	0.76
41	50	47.2	3.68	32.1	14.3	57.8	0.817
42	50	44.8	3.49	30.5	13.6	54.7	0.819
43	50	44	3.43	29.9	13.3	55.7	0.79
44	50	42.1	3.28	28.6	12.7	51.4	0.819
45	50	44.3	3.46	30.2	13.5	55.5	0.798

46	50	45.8	3.57	31.2	13.9	60.4	0.758
47	50	41	3.2	27.9	12.4	55.4	0.74
48	50	45	3.51	30.6	13.6	47.3	0.951
49	50	35.8	2.79	24.4	10.9	53.6	0.668
50	50	45.4	3.54	30.9	13.8	53.3	0.852
51	50	45.1	3.52	30.7	13.7	55.4	0.814
52	50	44	3.43	29.9	13.3	62	0.71
53	50	44.9	3.5	30.6	13.6	48.7	0.922
54	50	46.3	3.61	31.5	14	55.5	0.834
55	50	45.6	3.56	31.1	13.9	57.1	0.799
56	50	41.9	3.27	28.5	12.7	60.6	0.691
57	50	40.9	3.19	27.8	12.4	58.2	0.703
58	50	44.6	3.48	30.4	13.5	53.3	0.837
59	50	47.3	3.69	32.2	14.3	49.8	0.95
60	50	43.5	3.39	29.6	13.2	51.3	0.848

Peak Tube Voltage (kVp)	**Average Dose (mGy)**	**Average TAR**	**Average Kerma (mGy)**	**Average Dose per unit Kerma (mGy mGy^{-1})**
50	13.2	0.777	29.7	0.444

Table 2: Data acquired with Micro-CT X-Ray Tube Filter Thickness of 0.50 mm

TLD	Peak Tube Voltage (kVp)	Reading (nC)	Converted Exposure (R)	Calculated Air Kerma (mGy)	Calculated Dose (mGy)	In-Air Reading (nC)	TAR
1	70	80.8	7.5	65.5	57.1	76.4	1.06
2	70	79.5	7.4	64.6	56.3	78.8	1.01
3	70	77.6	7.2	62.9	54.8	64.2	1.21
4	70	77.9	7.2	62.9	54.8	79.2	0.984
5	70	80.9	7.5	65.5	57.1	72.7	1.11
6	70	79.7	7.4	64.6	56.3	76.6	1.04
7	70	72.1	6.7	58.5	51	75.7	0.952
8	70	79.1	7.4	64.6	56.3	72.2	1.1
9	70	77.9	7.2	62.9	54.8	73.8	1.06
10	70	82.5	7.7	67.2	58.6	76.4	1.08
11	70	79.9	7.4	64.6	56.3	75.2	1.06
12	70	71.1	6.6	57.6	50.2	73.5	0.967
13	70	76.7	7.1	62	54	78.5	0.977
14	70	69.3	6.4	55.9	48.7	77.7	0.892
15	70	79.5	7.4	64.6	56.3	78.9	1.01
16	70	82.4	7.7	67.2	58.6	67.8	1.22
17	70	77	7.2	62.9	54.8	77.1	1
18	70	67.1	6.2	54.1	47.2	76.4	0.878
19	70	73.7	6.9	60.2	52.5	69.2	1.07
20	70	69.7	6.5	56.7	49.4	78.9	0.883
21	70	80.3	7.5	65.5	57.1	77.5	1.04
22	70	86.1	8	69.8	60.8	75	1.15

23	70	66.4	6.2	54.1	47.2	75.4	0.881
24	70	75	7	61.1	53.3	77.3	0.97
25	70	83.2	7.7	67.2	58.6	77.5	1.07
26	70	80.6	7.5	65.5	57.1	78.7	1.02
27	70	86.3	8	69.8	60.8	75	1.15
28	70	73.3	6.8	59.4	51.8		
29	70	70.5	6.6	57.6	50.2		
30	70	74.1	6.9	60.2	52.5		
31	60	59.1	5.2	45.4	37.9	57.3	1.03
32	60	55	4.84	42.3	35.4	57.5	0.96
33	60	60.4	5.32	46.4	38.8	59	1.02
34	60	55.3	4.87	42.5	35.5	60	0.92
35	60	62.8	5.53	48.3	40.4	57.2	1.1
36	60	54.9	4.83	42.2	35.3	58.1	0.94
37	60	56.8	5	43.7	36.5	57.9	0.98
38	60	62	5.46	47.7	39.9	57	1.09
39	60	62.3	5.48	47.8	39.9	57.5	1.08
40	60	58.8	5.17	45.1	37.7	54.2	1.08
41	60	62.3	5.48	47.8	39.9	56.4	1.1
42	60	60.4	5.32	46.4	38.8	51.1	1.18
43	60	60.2	5.3	46.3	38.7	57	1.06
44	60	62	5.46	47.7	39.9	59.3	1.05
45	60	61.3	5.39	47.1	39.4	58.3	1.05
46	60	64.6	5.68	49.6	41.5	59.8	1.08
47	60	60	5.28	46.1	38.5	59.2	1.01
48	60	58.8	5.17	45.1	37.7	59.6	0.99

49	60	55.2	4.86	42.4	35.4	57.4	0.96
50	60	61.4	5.4	47.1	39.4	51.7	1.19
51	60	67.5	5.94	51.9	43.4	60.1	1.12
52	60	63.4	5.58	48.7	40.7	57.6	1.1
53	60	61.8	5.44	47.5	39.7	53.9	1.15
54	60	62.8	5.53	48.3	40.4	55.3	1.14
55	60	61.6	5.42	47.3	39.5	58.1	1.06
56	60	57.2	5.03	43.9	36.7	58.8	0.97
57	60	56.1	4.94	43.1	36	61.7	0.91
58	60	65.5	5.76	50.3	42	63.2	1.04
59	60	58.2	5.12	44.7	37.4		
60	60	59.8	5.26	45.9	38.4		
61	50	38	3.91	34.1	15.2	36.8	1.03
62	50	42.1	4.34	37.9	16.9	35.6	1.18
63	50	43.6	4.49	39.2	17.5	35.9	1.21
64	50	43.2	4.45	38.8	17.3	37.2	1.16
65	50	44.7	4.6	40.2	17.9	30.8	1.45
66	50					33.7	
67	50	44	4.53	39.5	17.6	30.2	1.46
68	50	41.6	4.28	37.4	16.7	33.2	1.25
69	50	36.8	3.79	33.1	14.7	36.7	1
70	50	43.8	4.51	39.4	17.5	34.6	1.27
71	50	40.9	4.21	36.8	16.4	30.1	1.36
72	50	42.5	4.38	38.2	17	35.7	1.19
73	50	41.9	4.32	37.7	16.8	32.7	1.28
74	50	40	4.12	36	16	36.3	1.1

75	50	42.4	4.37	38.2	17	42	1.01
76	50	37	3.81	33.3	14.8	30.6	1.21
77	50	44.1	4.54	39.6	17.6	34.3	1.29
78	50	40.4	4.16	36.3	16.2	35.5	1.14
79	50	43.8	4.51	39.4	17.5	35.4	1.24
80	50	43.7	4.5	39.3	17.5	35.5	1.23
81	50	40.8	4.2	36.7	16.3	31.3	1.3
82	50	43.4	4.47	39	17.4	35.9	1.21
83	50	41.5	4.27	37.3	16.6	33.2	1.25
84	50	41.2	4.24	37	16.5	34.2	1.2
85	50	40.8	4.2	36.7	16.3	35.1	1.16
86	50	41.5	4.27	37.3	16.6	36.7	1.13
87	50	43.8	4.51	39.4	17.5	32	1.37
88	50	44.1	4.54	39.6	17.6	58.3	0.76
89	50	38.3	3.94	34.4	15.3	51.7	0.74
90	50	46.2	4.76	41.6	18.5	52.5	0.88

Peak Tube Voltage (kVp)	**Average Dose (mGy)**	**Average TAR**	**Average Kerma (mGy)**	**Average Dose Per Unit Kerma (mGy mGy^{-1})**
70	54.5	1.03	62.5	0.872
60	38.7	1.05	46.3	0.836
50	16.8	1.17	37.7	0.446

Table 3: Data acquired with Micro-CT X-Ray Tube Filter Thickness of 1.0 mm

TLD	Peak Tube Voltage (kVp)	Reading (nC)	Converted Exposure (R)	Calculated Air Kerma (mGy)	Calculated Dose (mGy)	In-Air Reading (nC)	TAR
1	70	60.8	3.71	32.4	28.2	133.2	0.456
2	70	60.2	3.67	32	27.9	133.7	0.45
3	70	60.1	3.67	32	27.9	134.5	0.447
4	70	60.3	3.68	32.1	28	135.4	0.445
5	70	59.8	3.65	31.9	27.8	134.2	0.446
6	70	58.7	3.58	31.3	27.3	134.6	0.436
7	70	57.7	3.52	30.7	26.8	129.2	0.447
8	70	59.8	3.65	31.9	27.8	138.8	0.431
9	70	58.1	3.54	30.9	26.9	128.9	0.451
10	70	61.3	3.74	32.7	28.5	133.6	0.459
11	70	61.7	3.76	32.8	28.6		
12	70	53.4	3.26	28.5	24.8		
13	70	57.4	3.5	30.6	26.7		
14	70	51.6	3.15	27.5	24		
15	70	219.9					
16	70	59.5	3.63	31.7	27.6		
17	70	58.5	3.57	31.2	27.2		
18	70	51.1	3.12	27.2	23.7		
19	70	58.5	3.57	31.2	27.2		
20	70	55.7	3.4	29.7	25.9		
21	70	62.5	3.81	33.3	29		
22	70	64.5	3.93	34.3	29.9		

23	70	49.5	3.02	26.4	23		
24	70	56	3.42	29.9	26.1		
25	70	57.5	3.51	30.6	26.7		
26	70	58.7	3.58	31.3	27.3		
27	70	60.5	3.69	32.2	28.1		
28	70	52.1	3.18	27.8	24.2		
29	70	55.1	3.36	29.3	25.5		
30	70	56.5	3.45	30.1	26.2		
31	80	72.4	4.27	37.3	33.6		
32	80	70.8	4.18	36.5	32.9		
33	80	76.8	4.53	39.5	35.6		
34	80	68.4	4.04	35.3	31.8		
35	80	78.2	4.61	40.2	36.2		
36	80	73.5	4.34	37.9	34.1		
37	80	74.6	4.4	38.4	34.6		
38	80	74.9	4.42	38.6	34.7		
39	80	77.2	4.55	39.7	35.7		
40	80	81	4.78	41.7	37.5		
41	80	80.4	4.74	41.4	37.3		
42	80	75.3	4.44	38.8	34.9		
43	80	76.8	4.53	39.5	35.6		
44	80	77.5	4.57	39.9	35.9		
45	80	77.5	4.57	39.9	35.9		
46	80	73.6	4.34	37.9	34.1		
47	80	74.5	4.4	38.4	34.6		
48	80	74.2	4.38	38.2	34.4		

49	80	71.8	4.24	37	33.3		
50	80	82.8	4.89	42.7	38.4		
51	80	77.1	4.55	39.7	35.7		
52	80	80.3	4.74	41.4	37.3		
53	80	82.6	4.87	42.5	38.3		
54	80	80.2	4.73	41.3	37.2		
55	80	80.3	4.74	41.4	37.3		
56	80	74.4	4.39	38.3	34.5	162.6	0.458
57	80	72.7	4.29	37.5	33.8	153.7	0.473
58	80	84.2	4.97	43.4	39.1	175.5	0.48
59	80	79	4.66	40.7	36.6	167.3	0.472
60	80	79.7	4.7	41	36.9	168.1	0.474

Peak Tube Voltage (kVp)	**Average Dose (mGy)**	**Average TAR**	**Average Kerma (mGy)**	**Average Dose Per Unit Kerma (mGy mGy^{-1})**
80	35.6	0.471	39.5	0.873
70	26.9	0.447	30.8	0.901

Summary

After the discovery of X-rays in 1895, the field of medical imaging began to organize and a slew of new medical imaging devices were developed. While some developments occurred earlier, the computed tomography (CT or CAT for "computer automated tomography") scanner was not created until 1972 by Godfrey Hounsfield. The primary reason for the relatively late introduction of the modality was due to its dependence on the computer. The CT scan is completely digital; there is no meaningful image that results from an analysis of the raw data alone. The data, which is nothing more than a set of numbers called CT coefficients, must be analyzed and processed into an image through a process known as reconstruction which is done by the computer. The greatest advantage of CT is that the images it creates of the internal organs beneath the skin are incredibly detailed and three dimensional, providing physicians and researchers a powerful, noninvasive tool for modeling the internals of people. Today, the importance of computed tomography is difficult to exaggerate. It is the scan of choice preferred by physicians and researchers who wish to check for abnormalities of soft tissue and internal organs when making difficult diagnoses.

In such research, human subjects are typically not used. Rather, small animals such as mice and rats provide the ideal model for studies in biology, chemistry, and medicine. They provide a platform upon which new drug therapies can be developed and the timescale over which a small animal responds to such therapies is much shorter. For example, tumor growth in a human usually

occurs over a period of years. In a mouse, tumor growth occurs much more rapidly, over a period of days or even hours.

When computed tomography technology was introduced, researchers were excited to use the imaging technique on small animals but practical limitations made widespread adoption of CT technology virtually impossible. The main problem was one of scale; clinical CT scanners were simply too large to produce useful images of small animals. In order to apply the technology for use in research and small animals, a smaller-scale version of the scanners needed to be developed and the field of preclinical scanners was established.

It is important to consider the radiation dose to patient or subject when using any form of imaging modality which utilizes ionizing radiation (such as x-rays, as CT scanners do). Prolonged exposure to ionizing radiation can cause cancer if an ionized molecule interacts with and damages a molecule of DNA. Therefore, dosimetry studies, which measure the amount of dose which a patient is exposed to in certain scan conditions, are conducted on clinical scanners as part of routine maintenance and safety certification. Dose is the measure of energy which is absorbed by tissue following exposure to ionizing radiation, where exposure is the measure of ionizing radiation per unit mass of air irradiated. A way to imagine the difference between exposure and dose is to consider x-rays as rain drops. Exposure is the measure of "rain" falling on and around the irradiated object, such as your hand for example, whereas dose is the amount of "water" which (somehow, perhaps through the sweat glands) is absorbed into the skin. Unfortunately, obtaining a direct measure of dose would be seemingly impossible,

requiring instruments to be placed within living tissue. However, measuring exposure is much more practical and fortunately, for the purposes of this study, the exposure and dose are directly related through air kerma (kinetic energy released in matter) by a conversion factor known as the *f-factor* which is uniform throughout the small animal.

The instrument used to measure exposure is the ionization chamber. The chamber contains a tip in which a parallel plate capacitor is housed. As ionizing radiation interacts with and ionizes air molecules, the positively charged air molecule will tend towards the negatively charged plate, whereas the liberated electron will be attracted towards the positive plate. This movement can then be detected and reported as a measure of current, which is the movement of electrons, per unit mass of air irradiated. Typically this measurement is small, and the conventional unit is known as the roentgen (R), where $1\ R = 2.58 \times 10^{-4}$ C/kg.

Alas, another issue to consider arises. The ionization chamber tip is relatively large in diameter (compared to a small animal) and impossible to implant within a specimen, so direct measurement of exposure cannot be made. Instead, devices known as thermoluminescent dosimeters (TLDs) are used. The composition of the TLD chip material itself is such that electrons which interact with the chip become trapped and are released (*luminescence*) only by heating (*thermo*). Another benefit of TLD chips is that they are very small, and easily placed in phantoms (objects which are constructed out of material which interacts with ionizing radiation in a manner similar to that of tissue).

While the dosimetry study is commonplace in the clinical setting, it is not performed regularly in the preclinical setting and until this project, only theoretical predictions of dose to small animals existed. Empirical estimates were desired in order to evaluate the predictions and also provide researchers with the tools necessary in order to more confidently account for the dose imparted to their specimens during scanning. For example, a researcher studying the effects of radiation therapy on tumor growth in a mouse may require daily use of the micro-CT scanner. They would need to account for the dose the mouse received during scanning as a non-trivial source of radiation therapy in itself. Therefore, when the SUNY Upstate Medical University purchased a preclinical CT (micro-CT) scanner, a dosimetry study was conducted.

The dosimetry study was performed as follows. As a preliminary step, the TLDs were calibrated so that when read, the output of the ammeter (used to read the TLDs) could be converted into measurements of exposure. This was accomplished by exposing a set of 30 TLDs (3 scans of 10 TLDs each) outside of any phantom (in air) and then exposing the ionization chamber in identical conditions (known as technique). The measurements reported by the ionization chamber were then averaged and the TLDs were then read. Conversion factors relating the output of the ammeter into measurements of exposure as reported by the ionization chamber were then calculated. The TLDs were then annealed and a new set of scans was performed utilizing the same technique except that the TLDs were placed inside of a mouse phantom. The TLDs were then read, their readings converted into measurements of exposure and air kerma, and the final calculation

of dose was made. This process was repeated for technique commonly used in the small animal scans, with the result being a series of equations. The equations allow researchers to input their desired scan technique and the result is an empirically-derived estimate of the dose to the small animal.

The significance of this project was that it resulted in an empirically-derived dose estimate model. Such a model has many uses, with the primary use being that it predicts the dose to an animal during a scan. As a secondary application, these dose predictions will be used to evaluate a new method of x-ray generation currently under development by the SMIRG which may eventually be used in industry. The theory is that the new method is believed to result in shorter scans, lower patient dose, and higher resolution images. The model developed as a result of this project will be used to evaluate the claim of lower dose. By using the same procedure, a similar study will be conducted and the results will be compared to evaluate if in fact dose is reduced.